Electronic Supplementary Material (ESI) for Environmental Science: Water Research & Technology.
This journal is © The Royal Society of Chemistry 2022

Role of co-existing anions in non-radical and radical processes of carbocatalyzed persulfate activation for acetaminophen degradation

Kadarkarai Govindan[a], Do-Gun Kim[b], Seok-Oh Ko[a, *]

[a] Environmental System Laboratory, Department of Civil Engineering, Kyung Hee University-Global Campus, 1732 Deogyeong-daero, Giheung-Gu, Yongin-Si, Gyeonggi-Do 16705, Republic of Korea

[b] Department of Environmental Engineering, Sunchon National University, 255 Jungang-ro, Suncheon, Jellanam-do, 57922, Republic of Korea

* **Corresponding authors:**

Email: soko@khu.ac.kr (Seok-Oh Ko)

Text S1. Materials

Multiwalled carbon nanotubes (MWCNT) with a diameter of 5-15 nm and length of ~10 μm were purchased from Carbon Nano-Materials Technology Co., Ltd., South Korea. Dicyandiamide (99.5%, $C_2H_4N_4$, 81.08 g mol^{-1}) and ethyl alcohol (99.5%, C_2H_5OH), were purchased from Sigma Aldrich, South Korea. Potassium persulfate (PS, K_2S_2O8, 270.32 g mol^{-1}), sodium hydroxide (NaOH, 40 g mol^{-1}), sodium chloride (NaCl, 58.44 g mol^{-1}), sodium sulfate (Na_2SO_4 142.04 g mol^{-1}), sodium nitrate ($NaNO_3$ 84.99 g mol^{-1}), sodium carbonate (Na_2CO_3, 105.99 g mol^{-1}), and sodium bicarbonate ($NaHCO_3$, 84.01 g mol^{-1}) were received from SamChun Chemicals, South Korea. All chemicals were laboratory grade and were used without further purifications. In addition, HPLC grade methanol (99%, CH_3OH, 32.04 g mol^{-1}) for HPLC was purchased from Honeywell, South Korea.

Text S2. Characterizations

The crystalline nature and structural deformation of the as-synthesized N-MWCNT were gathered using high resolution Raman spectroscopy (InVia Raman microscopes) and a powder X-ray diffractometer (XRD, D8 Advance Bruker) analysis. From the XRD results, the interlayer distance of the graphitic plane was determined by Bragg's equation, $n\lambda = 2d\sin\theta$, where λ is the incident wavelength (-1.5406 Å), θ is the peak position, n is the order of diffraction (1), and d is the interlayer spacing or d-spacing value. The chemical entity, its composition, and the structural defects density of the carbocatalyst were analyzed with a K-Alpha TM X-ray photoelectron spectrometer (XPS) system (ThermoFisher Scientific, USA) and all the XPS spectra were fitted by XPSSEAK 41 software. The surface topography was analyzed with high resolution transmission electron microscopy (HR-TEM, JEOL JEM-2100F). The point of zero charge (pH_{PZC}) of the carbon catalyst were measured using a zeta potential analyzer (ZetaPlus, Brookhaven, USA)

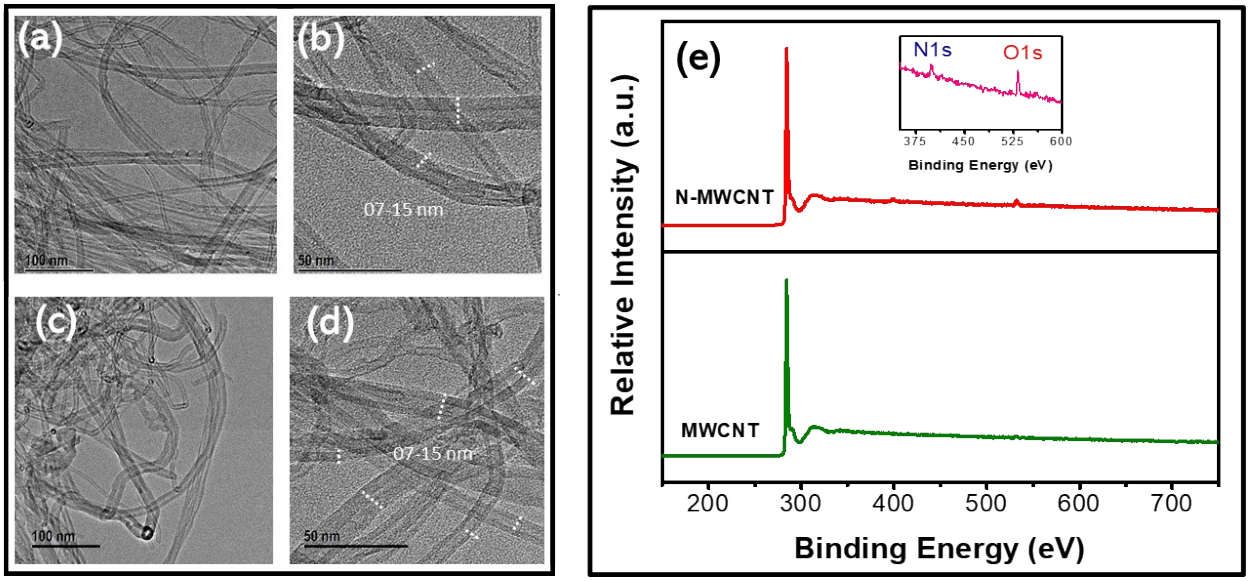

Fig. S1. HR-TEM images for pristine MWCNT (a, b) and N-MWCNT (c, d); (e) XPS full survey spectra of MWCNT and N-MWCNT, N 1s signal (Insert figure).

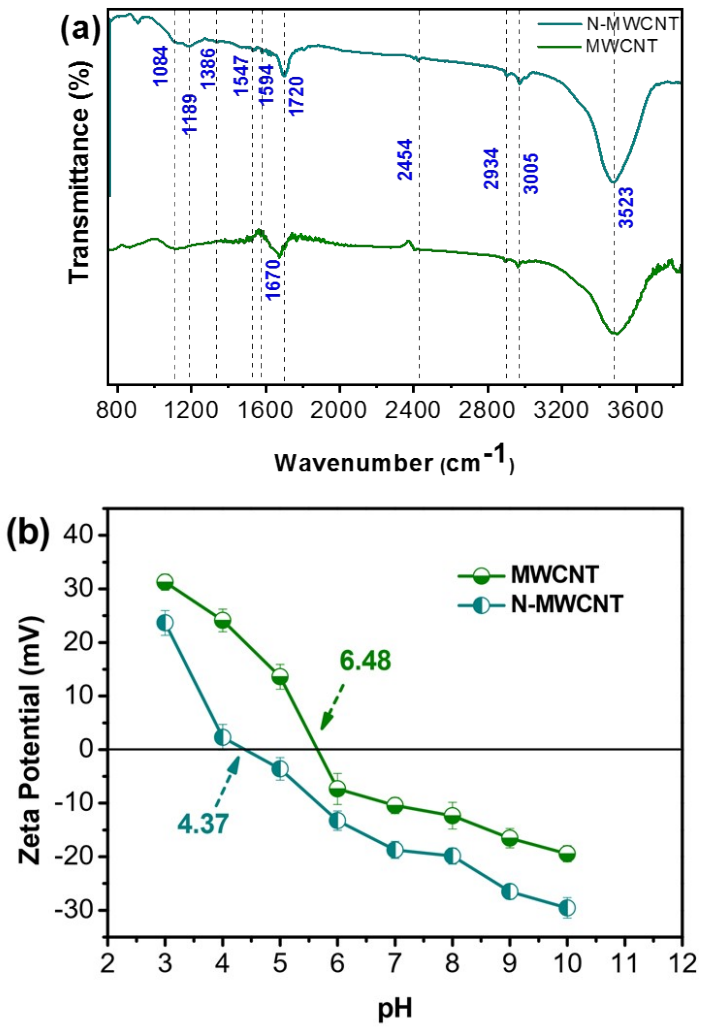
(a)
N-MWCNT
MWCNT
1084
1189
1386
1547
1594
1720
2454
2934
3005
3523
1670
Transmittance (%)
800 1200 1600 2000 2400 2800 3200 3600
Wavenumber (cm-1)
(b)
MWCNT
N-MWCNT
6.48
4.37
Zeta Potential (mV)
40 30 20 10 0 -10 -20 -30
2 3 4 5 6 7 8 9 10 11 12
pH

Fig. S2. FT-IR spectra and (b) Zeta potential of MWCNT and N-MWCNT under different pH conditions

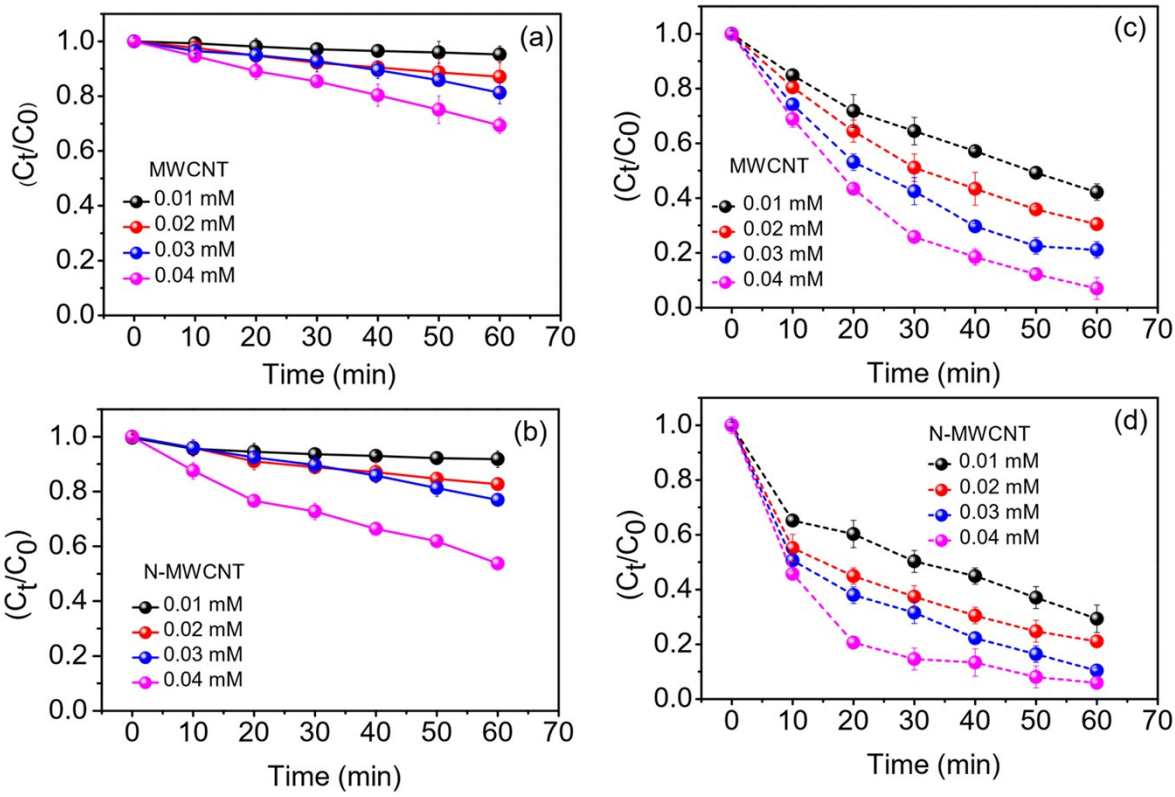

Fig. S3. Effect of PS dosage on normalized concentration of ACP (a, b) and normalized PS concentration (c, d). Experimental conditions were C_{ACP} = 10 mg L^{-1}, $C_{Catalyst}$ = 100 mg L^{-1}, pH_i = 7.01 ± 0.2, and C_{PS} = 0.01, 0.02, 0.03, and 0.04 mM.

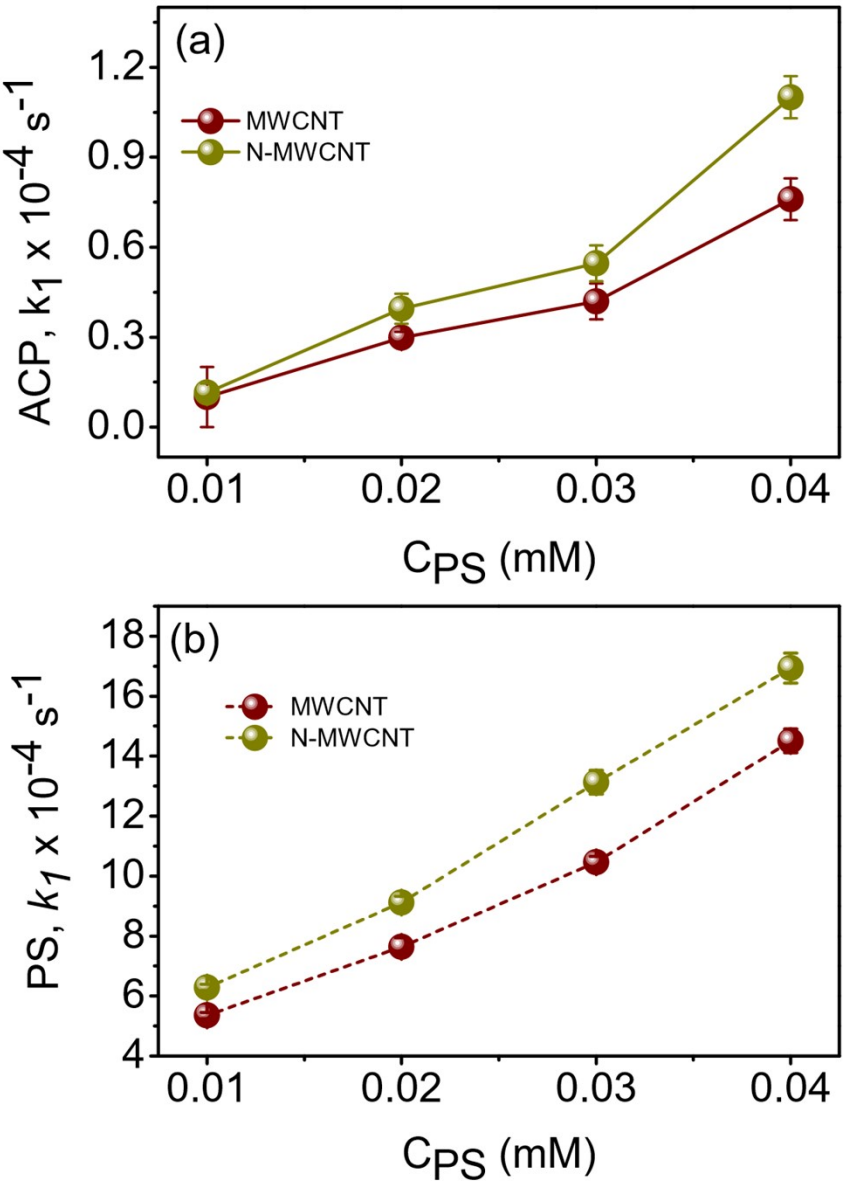

Fig. S4. Effect of PS dosage on ACP degradation rate constant and PS decomposition rate. Experimental conditions were C_{ACP} = 10 mg L^{-1}, $C_{Catalyst}$ = 100 mg L^{-1}, pH_i = 7.01 ± 0.2, and C_{PS} = 0.01, 0.02, 0.03, and 0.04 mM.

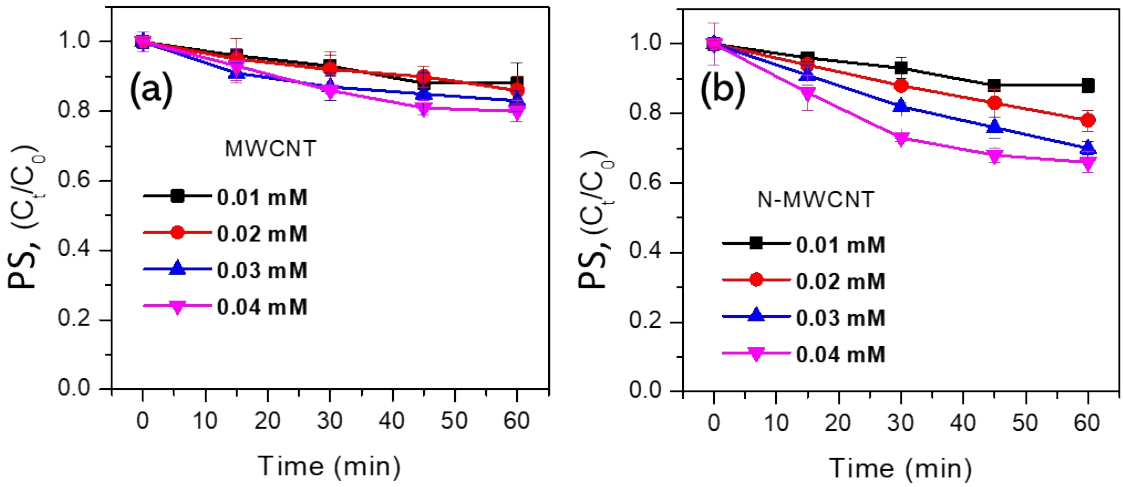

Fig. S5. PS adsorption efficiency at different PS dosage from (c) MWCNT/PS and (d) N-MWCNT/PS, without ACP. Experimental conditions were $C_{Catalyst}$ = 100 mg L^{-1}, and C_{PS} = 0.04 mM

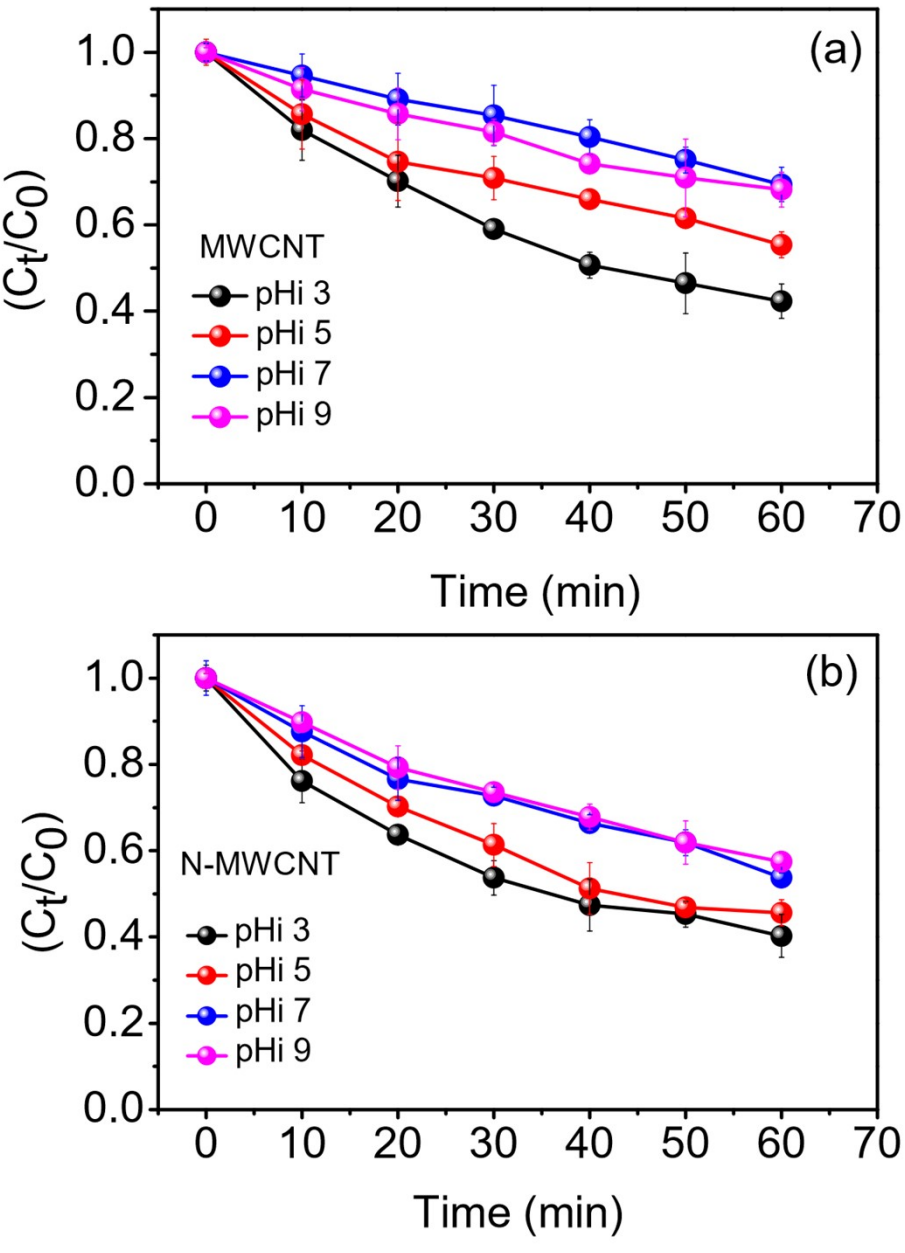

Fig. S6. Normalized concentration of ACP with different pH_i of the (a) MWCNT, (b) N-MWCNT catalytic system. Experimental conditions were C_{ACP} = 10 mg L^{-1}, $C_{Catalyst}$ = 100 mg L^{-1}, and C_{PS} = 0.04 mM.

.

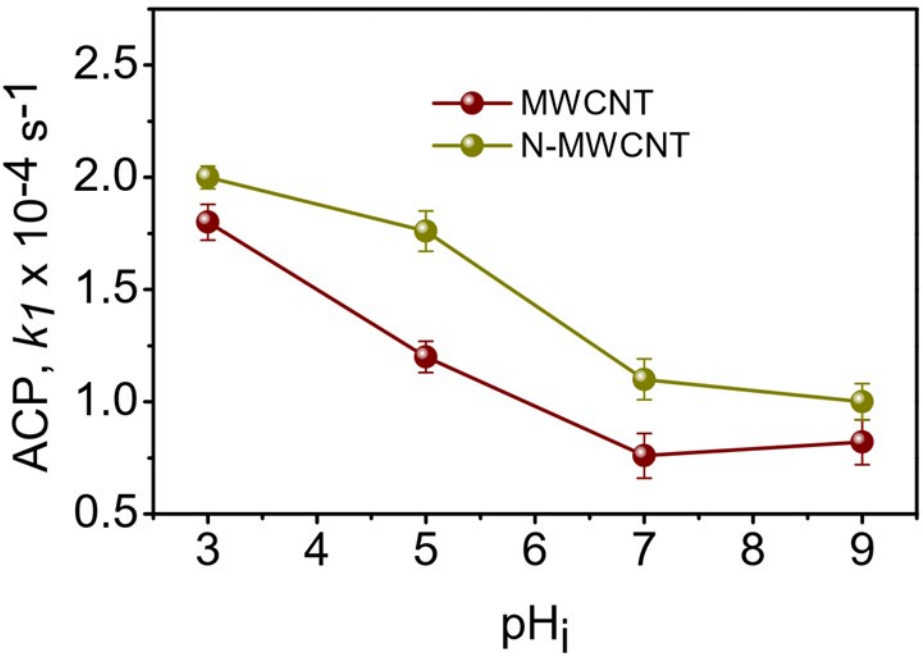

Fig. S7 Effect of pHi on ACP degradation rate constant. Experimental conditions were C_{ACP} = 10 mg L^{-1}, $C_{Catalyst}$ = 100 mg L^{-1}, and C_{PS} = 0.04 mM.

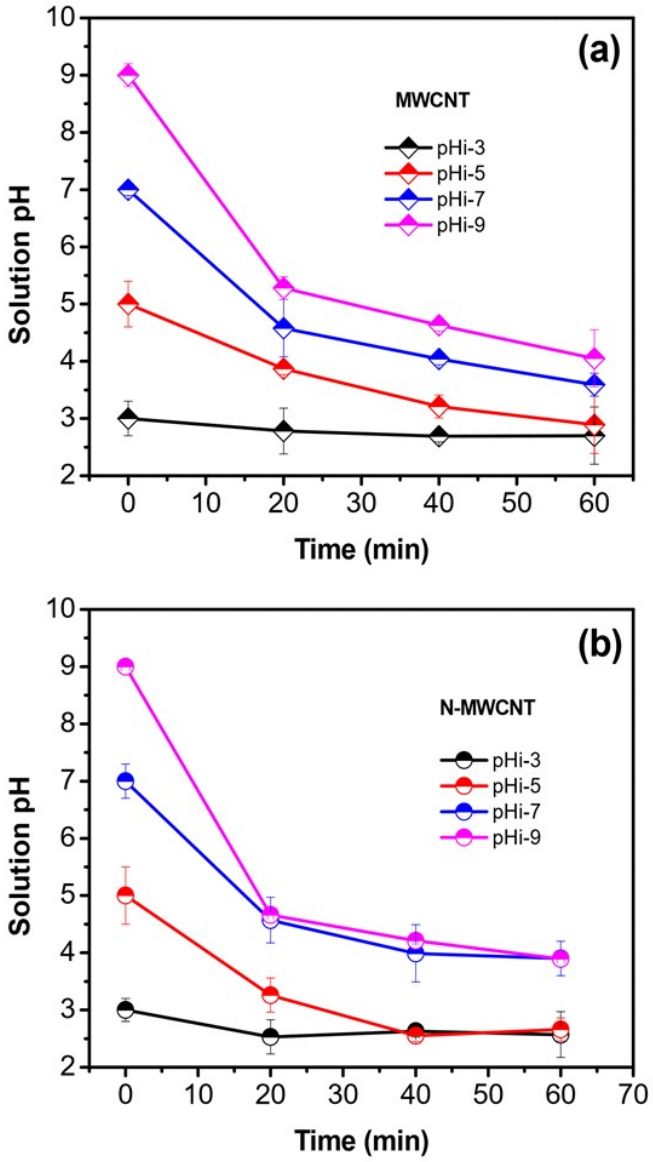

Fig. S8. Solution pH changes at different initial solution pH (a) MWCNT and (b) N-MWCNT

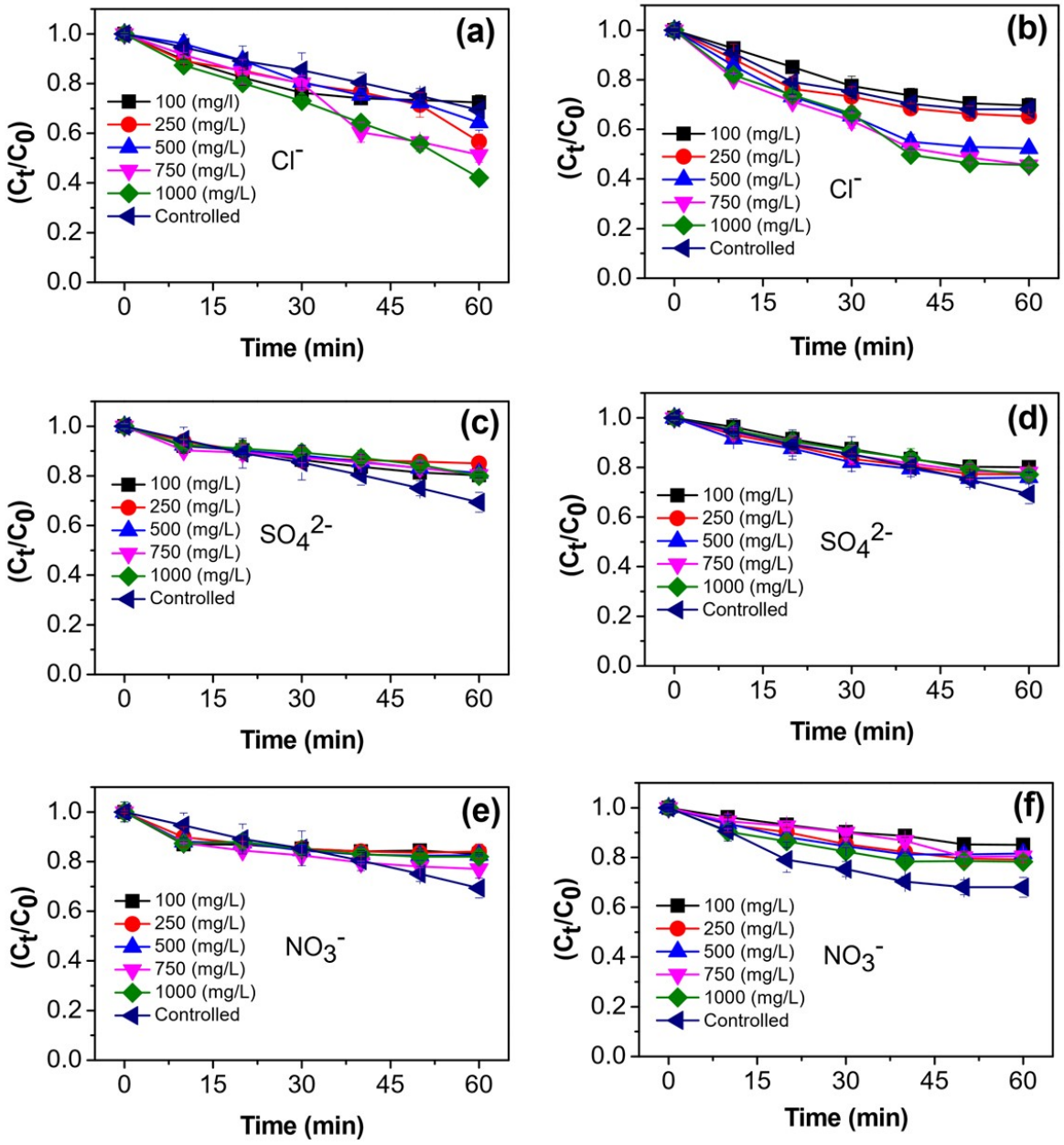

Fig. S9. Normalized concentration of ACP at MWCNT/PS (a, c, and e) and N-MWCNT/PS (b, d, and f) with different Cl^- (a-b), SO_4^{2-} (c-d), and NO_3^- (e-f) dosage. Experimental conditions were C_{ACP} = 10 mg L^{-1}, $C_{Catalyst}$ = 100 mg L^{-1}, C_{PS} = 0.04 mM, C_{anions} = 100, 250, 500, 750, and 1000 mg L^{-1}, and pH_i = 7.01 ± 0.2.

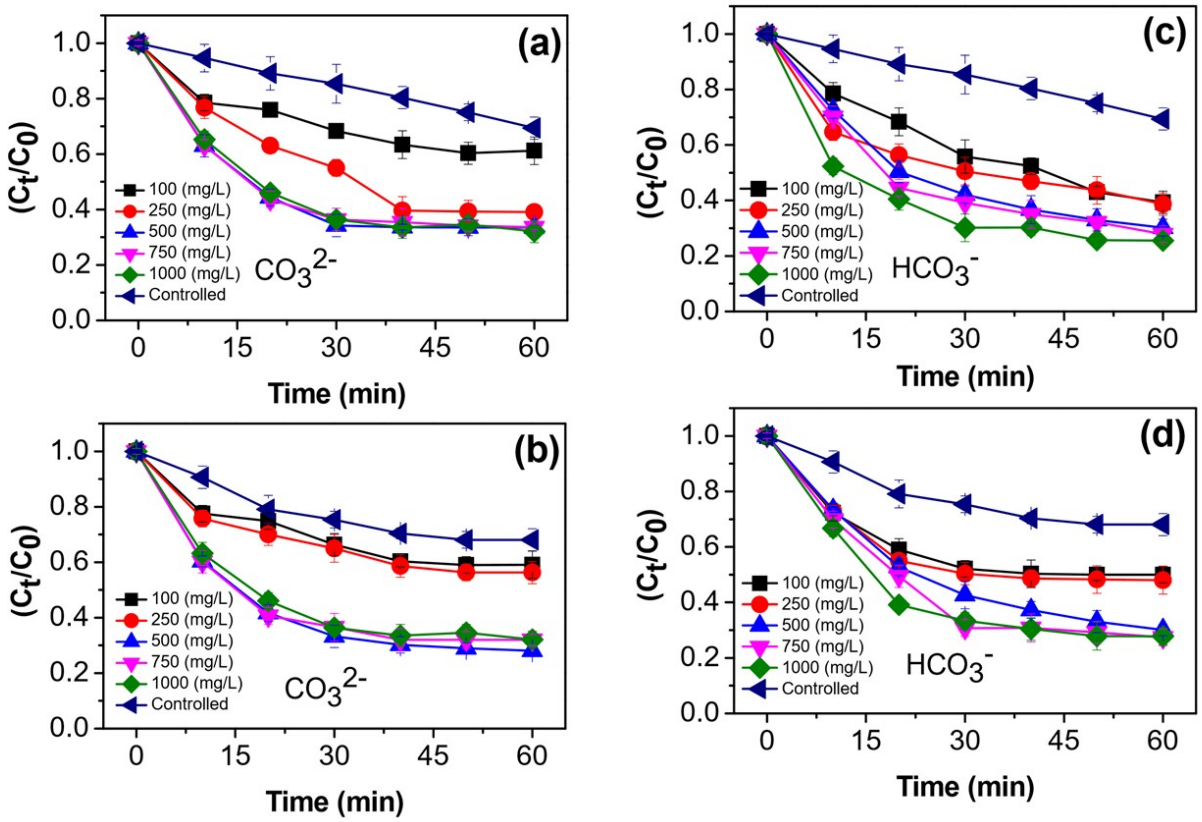

Fig. S10. Normalized concentration of ACP at MWCNT/PS (a and c) and N-MWCNT/PS (b and d) with different CO_3^{2-} (a-b) and HCO_3^- (c-d) dosage. Experimental conditions were C_{ACP} = 10 mg L^{-1}, $C_{Catalyst}$ = 100 mg L^{-1}, C_{PS} = 0.04 mM, C_{anions} = 100, 250, 500, 750, and 1000 mg L^{-1}, and pH_i = 7.01 ± 0.2.

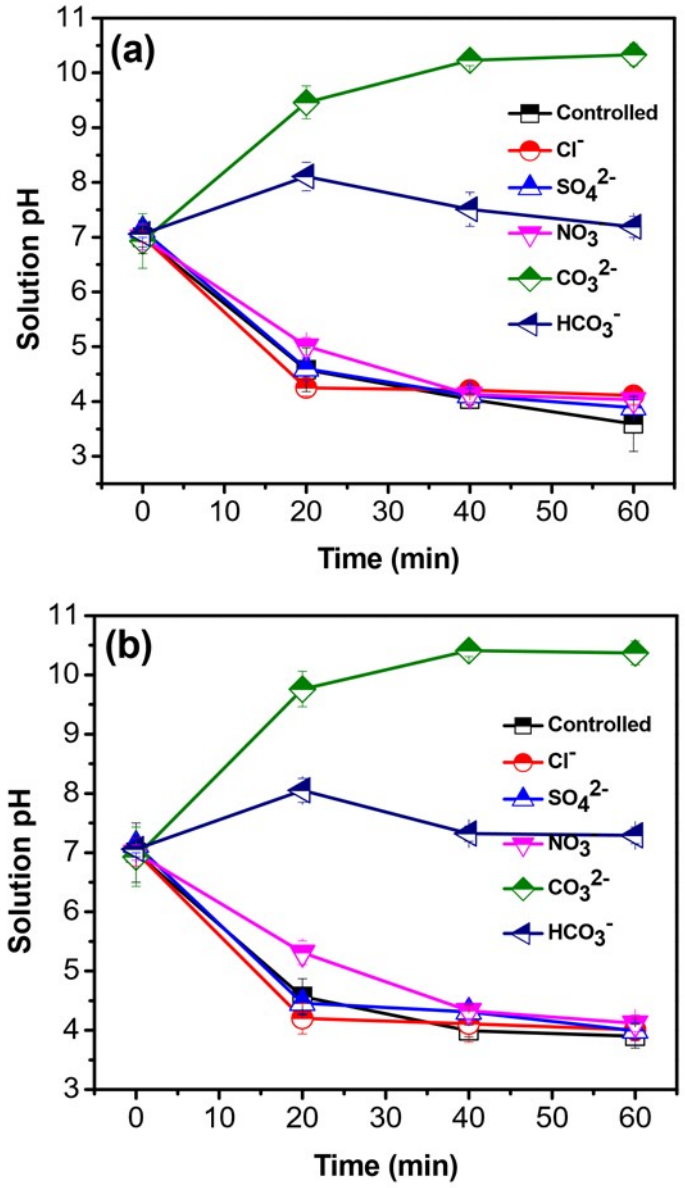

Fig. S11. Solution pH changes at co-exiting anions conditions (a) MWCNT and (b) N-MWCNT. Experimental conditions were C_{ACP} = 10 mg L^{-1}, $C_{Catalyst}$ = 100 mg L^{-1}, C_{PS} = 0.04 mM, C_{anions} = 500 mg L^{-1}, and pH_i = 7.01 ± 0.2.

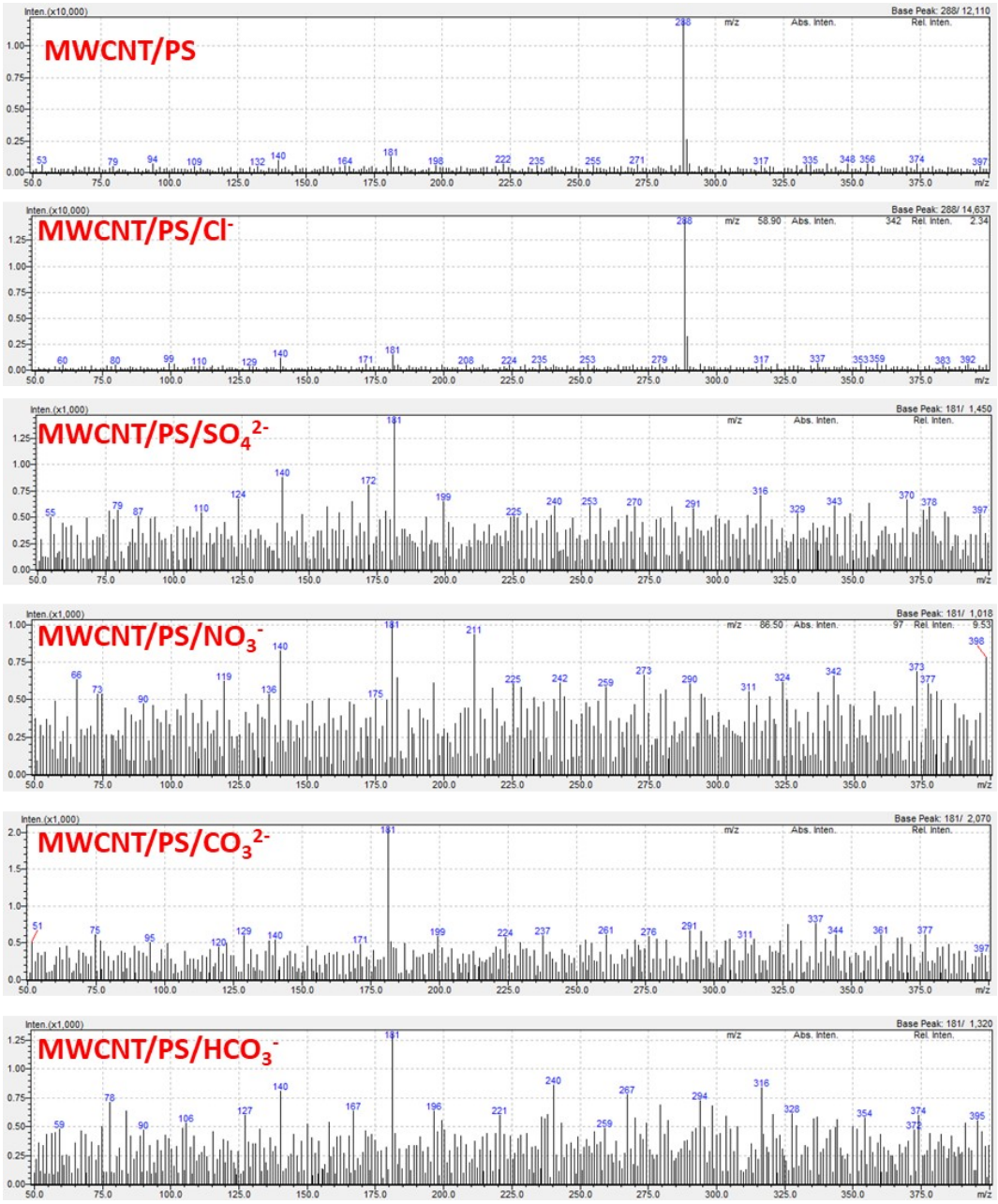

Fig. S12. LC-MS spectra obtained for different catalytic processes. Experimental conditions were $C_{Catalyst}$ = 100 mg L^{-1}, C_{ACP} = 10 mg L^{-1}, C_{PS} = 0.04 mM, $C_{co\text{-}existing\ ion}$ = 500 mg L^{-1} , and pH_i = 7.01 ± 0.2.

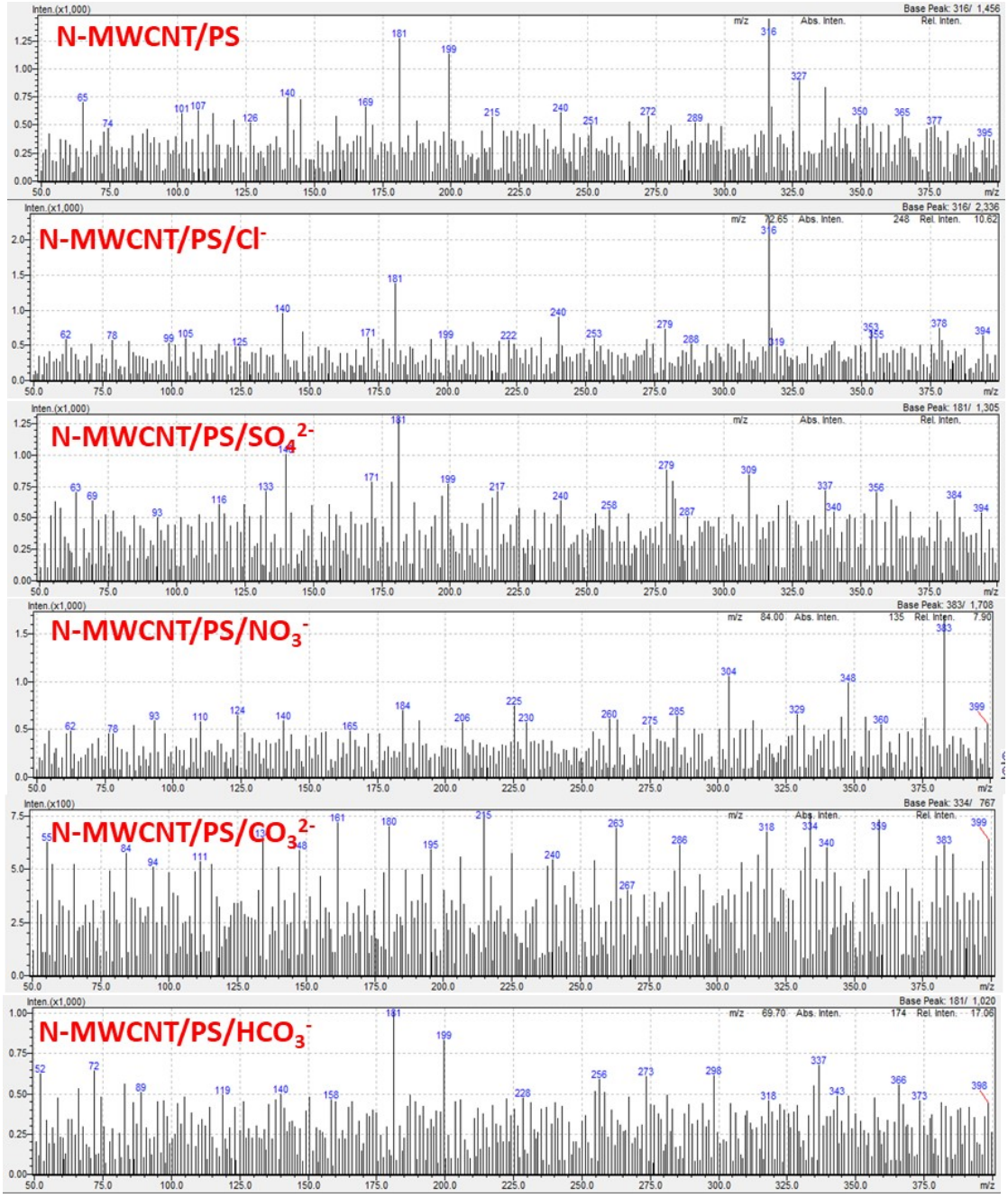

Fig. S13. LC-MS spectra obtained for different catalytic processes. Experimental conditions were $C_{Catalyst}$ = 100 mg L^{-1}, C_{ACP} = 10 mg L^{-1}, C_{PS} = 0.04 mM, $C_{co\text{-}existing\ ion}$ = 500 mg L^{-1} , and pH_i = 7.01 ± 0.2.

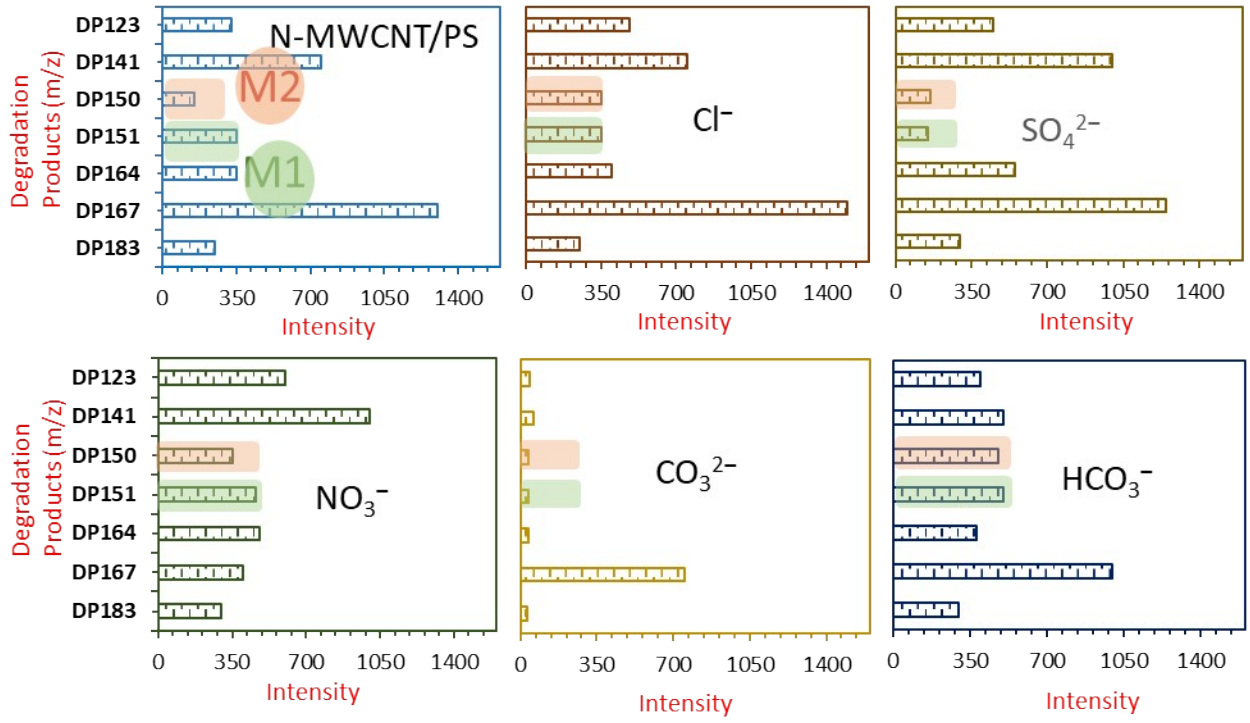

Fig. S14. Electron transfer initiated oxidative degradation products (m/z) by N-MWCNT/PS in the presence and absence of co-existing anions. Conditions: $C_{Catalyst}$ = 100 mg L^{-1}, C_{ACP} = 10 mg L^{-1}, C_{PS} = 0.04 mM, $C_{co\text{-}existing\ ion}$ = 500 mg L^{-1}, and pH_i = 7.01 ± 0.2.

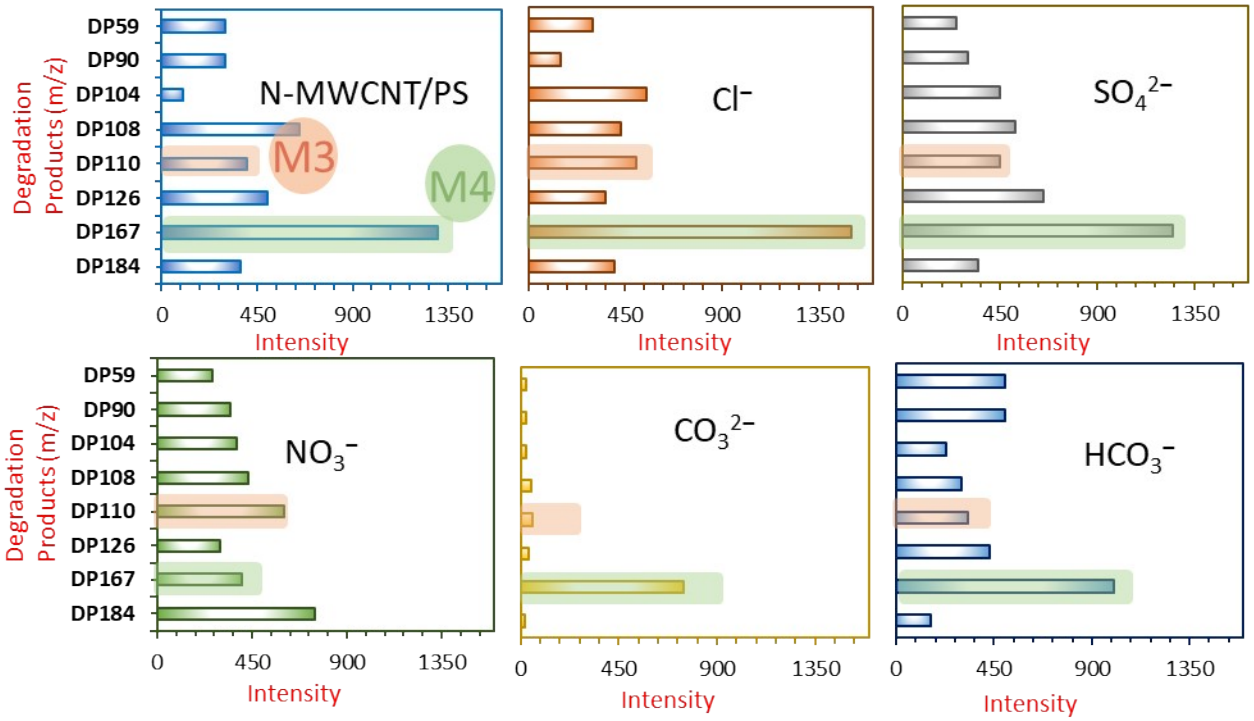

Fig. S15. Hydroxylation initiated oxidative degradation products (m/z) by N-MWCNT/PS in the presence and absence of co-existing anions. Conditions: $C_{Catalyst}$ = 100 mg L^{-1}, C_{ACP} = 10 mg L^{-1}, C_{PS} = 0.04 mM, $C_{co\text{-}existing\ ion}$ = 500 mg L^{-1}, and pH_i = 7.01 ± 0.2.

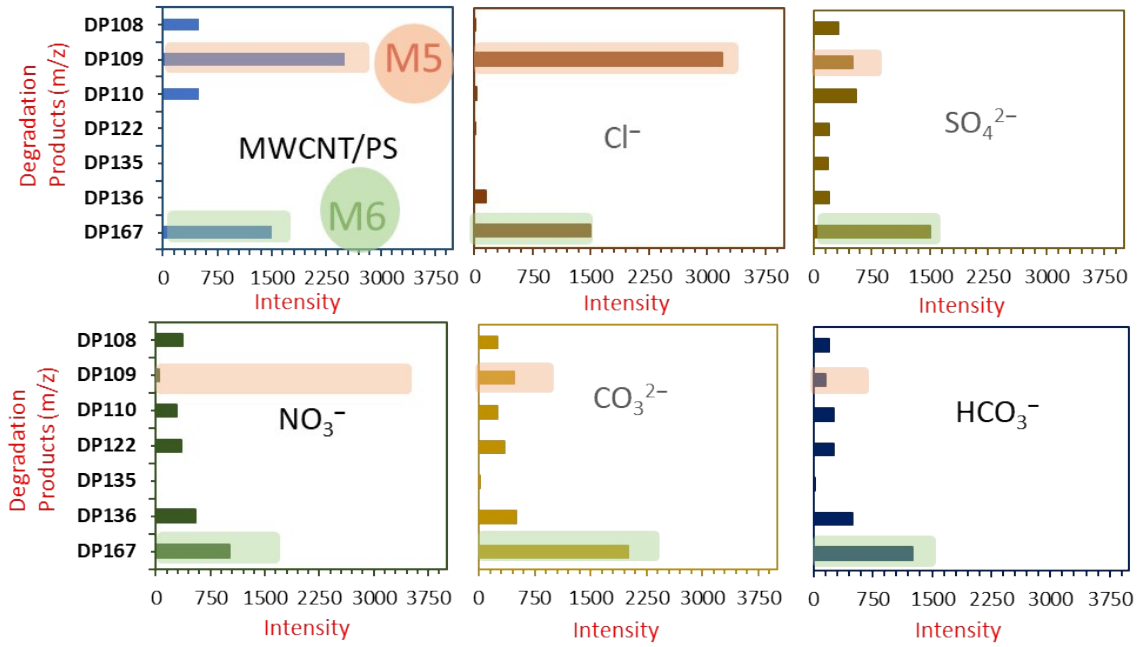

Fig. S16. Hydroxylation and ring opening oxidative degradation products (m/z) by MWCNT/PS in the presence and absence of co-existing anions. Conditions: $C_{Catalyst}$ = 100 mg L^{-1}, C_{ACP} = 10 mg L^{-1}, C_{PS} = 0.04 mM, $C_{co\text{-}existing\ ion}$ = 500 mg L^{-1}, and pH_i = 7.01 ± 0.2.

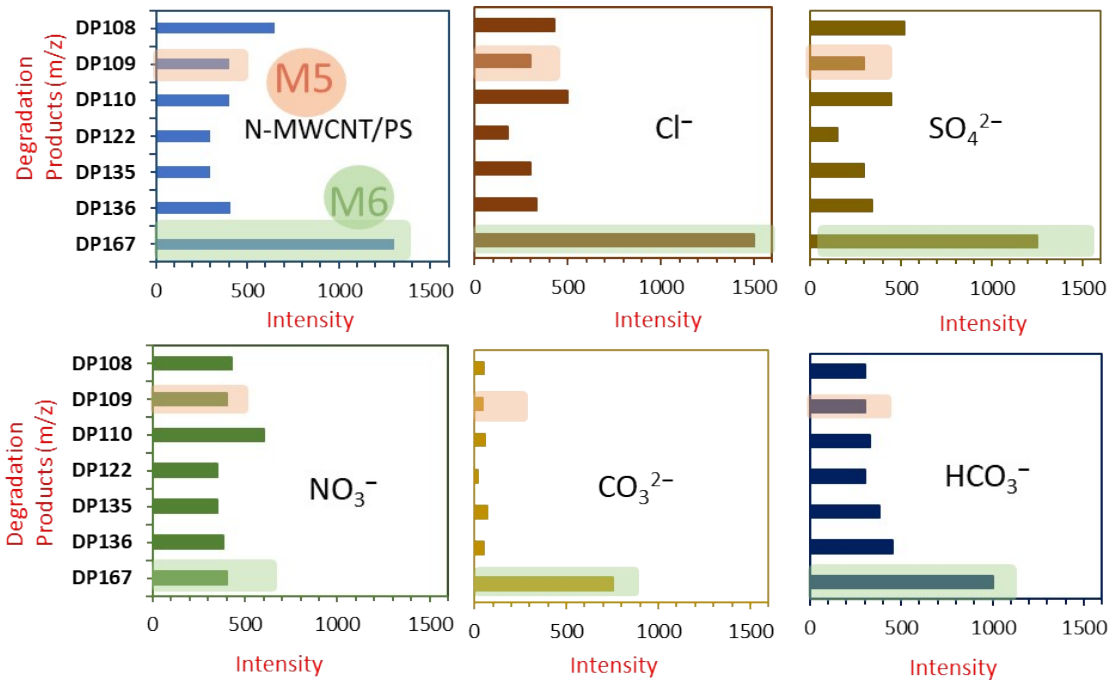

Fig. S17. Hydroxylation and ring opening oxidative degradation products (m/z) by N-MWCNT/PS in the presence and absence of co-existing anions. Conditions: $C_{Catalyst}$ = 100 mg L^{-1}, C_{ACP} = 10 mg L^{-1}, C_{PS} = 0.04 mM, $C_{co\text{-}existing\ ion}$ = 500 mg L^{-1}, and pH_i = 7.01 ± 0.2.